

Electronic Supplementary Information for:

Versatile organic photovoltaics with a power density of nearly 40 W g⁻¹

Xiangjun Zheng,^a Lijian Zuo,^{a,b} Kangrong Yan,^a Shiqi Shan,^a Tianyi Chen,^a Guanyu Ding,^a Bowei Xu,^c Xi Yang,^d Jianhui Hou,^c Minmin Shi,*^a and Hongzheng Chen*^a*

^a State Key Laboratory of Silicon Materials, MOE Key Laboratory of Macromolecular Synthesis and Functionalization, Department of Polymer Science and Engineering, Zhejiang University, Hangzhou 310027, P. R. China.

^b Zhejiang University-Hangzhou Global Scientific and Technological Innovation Center, Hangzhou 310014, P. R. China.

^c State Key Laboratory of Polymer Physics and Chemistry, Beijing National Laboratory for Molecular Sciences, Institute of Chemistry, Chinese Academy of Sciences, Beijing 100190, P. R. China.

^d ChasingLight Technology Co., Ltd, Guangzhou 510700, P. R. China

E-mail: zjuzlj@zju.edu.cn; minminshi@zju.edu.cn; hzchen@zju.edu.cn

Supplementary Figures

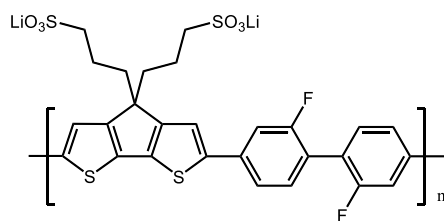


Figure S1. The chemical structure of PCP-2F-Li

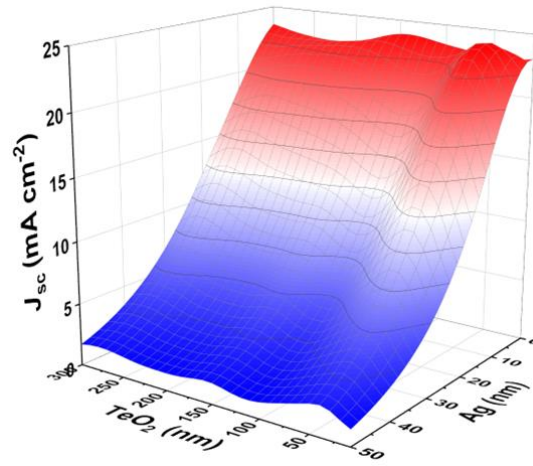


Figure S2. Optical simulation results of the ultra-thin Ag and TeO_2 thickness-dependent J_{sc} .

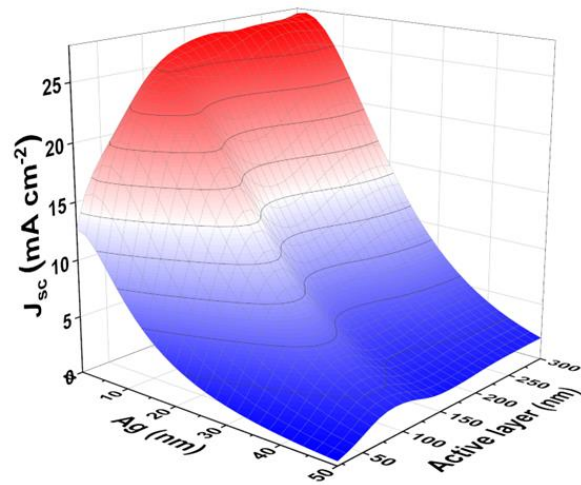


Figure S3. Optical simulation results of the ultra-thin Ag and active layer thickness-dependent J_{sc} .

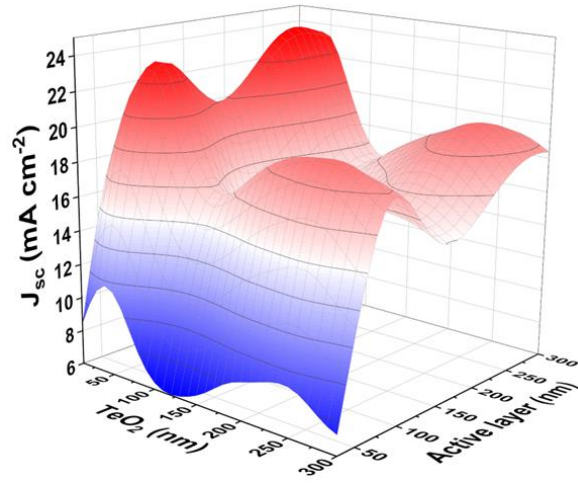


Figure S4. Optical simulation results of the active layer and TeO_2 thickness-dependent J_{sc} .

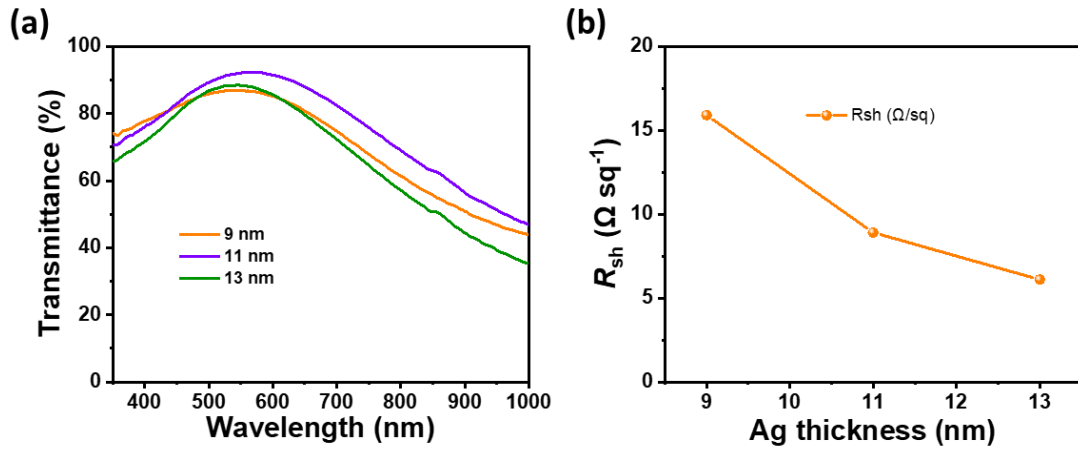


Figure S5. (a) Transmittances and (b) sheet resistances of ultra-thin Ag films with different thicknesses.

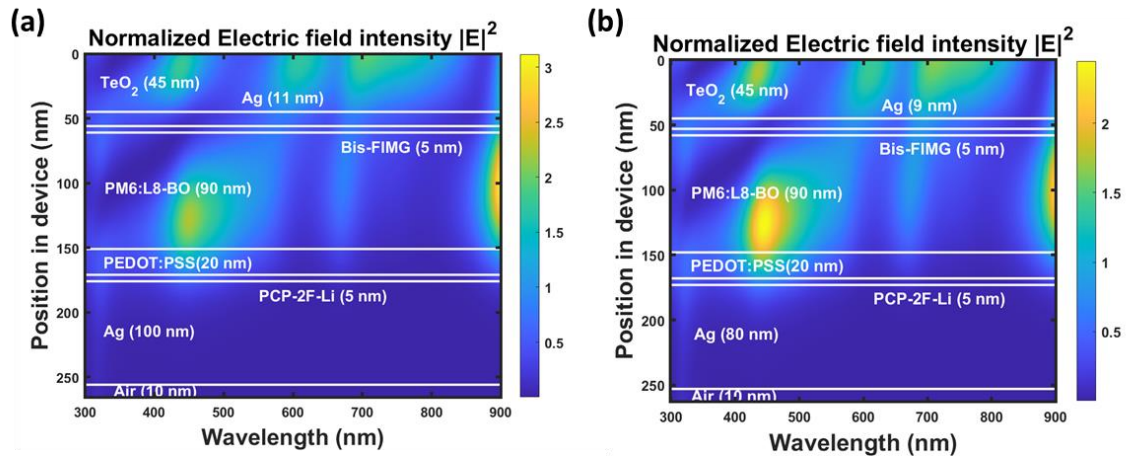


Figure S6. Optical simulation results of optical micro-cavity in the device chamber based on (a) 11 nm and (b) 9 nm ultra-thin Ag.

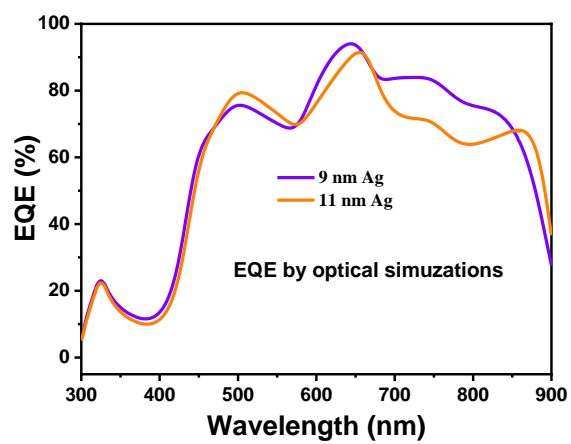


Figure S7. EQE spectra obtained by optical simulations based on 9 nm and 11 nm ultra-thin Ag films.

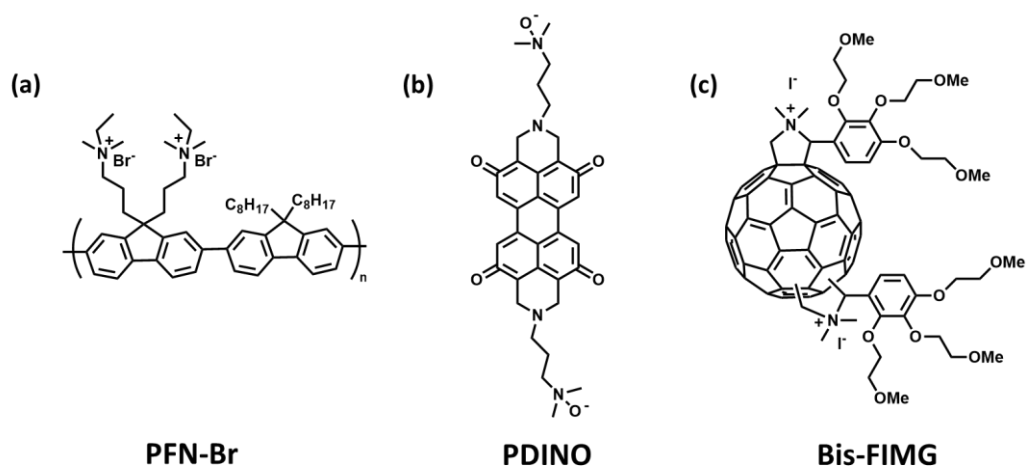


Figure S8. The chemical structures of (a) PFN-Br, (b) PDINO and (c) Bis-FIMG.

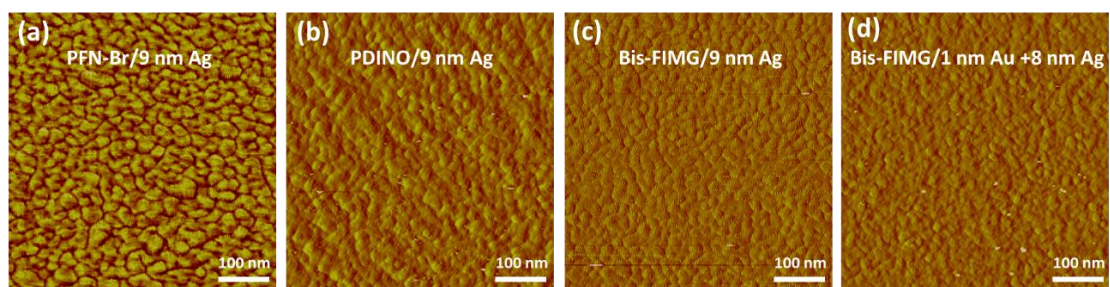


Figure S9. The phase images of (a) PFN-Br/9 nm Ag, (b) PDINO/9 nm Ag, (c) Bis-FIMG/9 nm Ag and (d) Bis-FIMG/1 nm Au/8 nm Ag films.

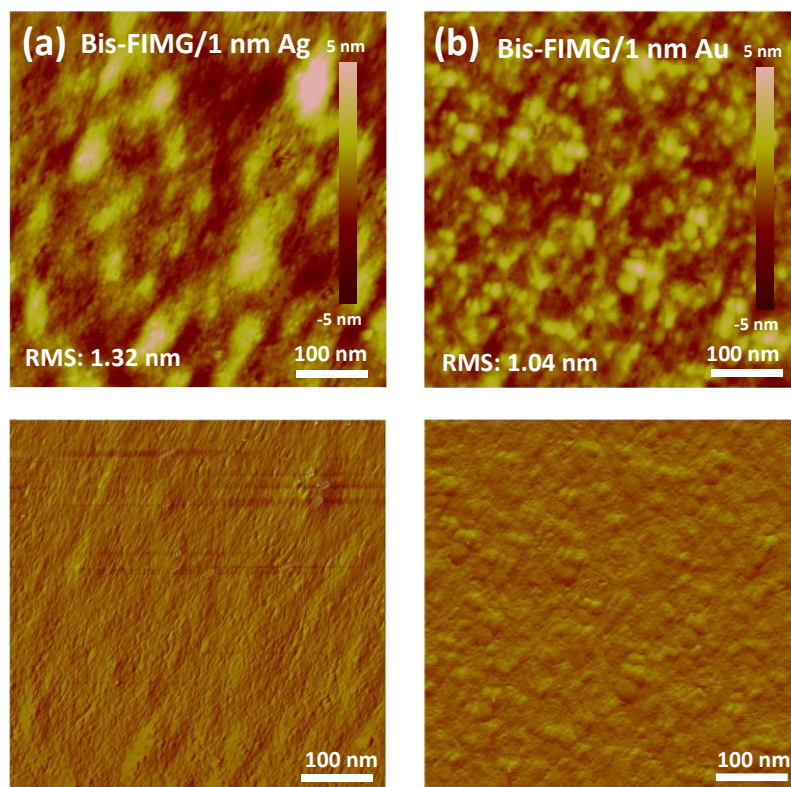


Figure S10. The AFM images (top: height, bottom: phase) of (a) Bis-FIMG/1 nm Ag, (b) Bis-FIMG/1 nm Au films.

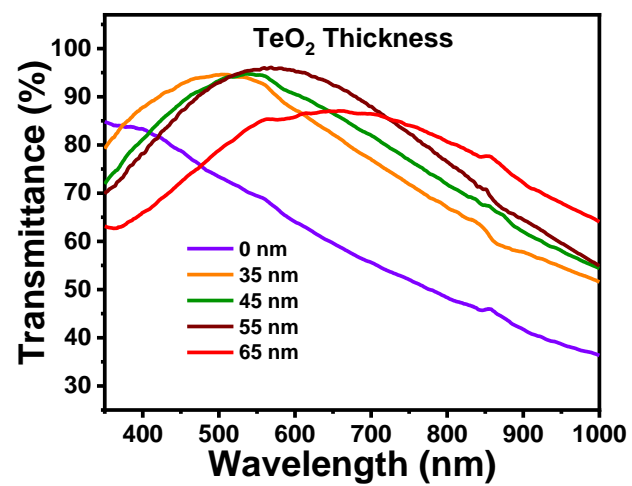


Figure S11. The transmittances of 0 nm, 35 nm, 45 nm, 55nm and 65 nm TeO₂ films.

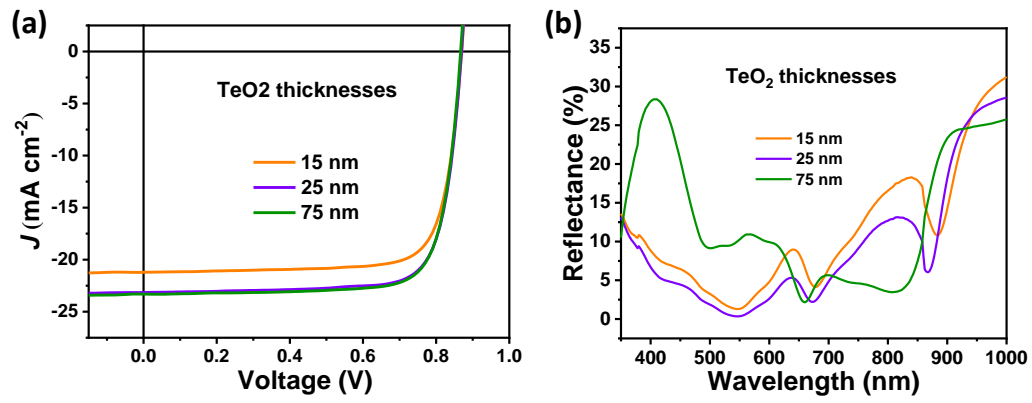


Figure S12. (a) J-V characteristics and (b) reflectance spectra of TUA-based devices with 15 nm, 25 nm and 75 nm TeO₂.

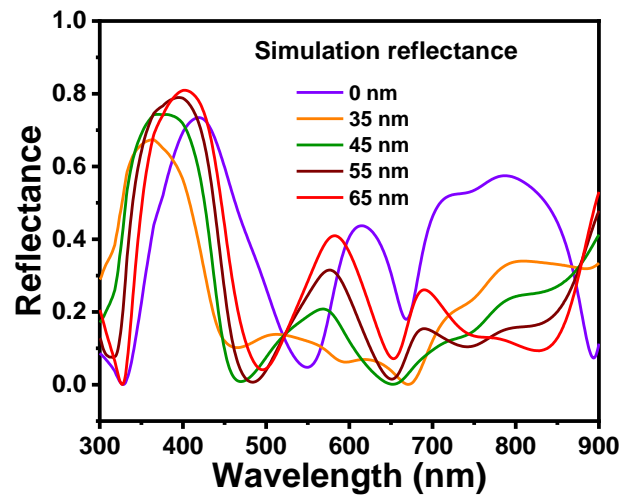


Figure S13. The simulated optical reflectance of 0 nm, 35 nm, 45 nm, 55nm and 65 nm TeO₂ based OPV devices.

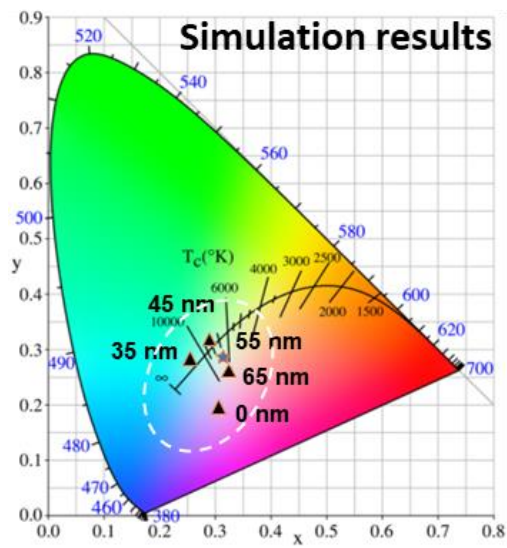
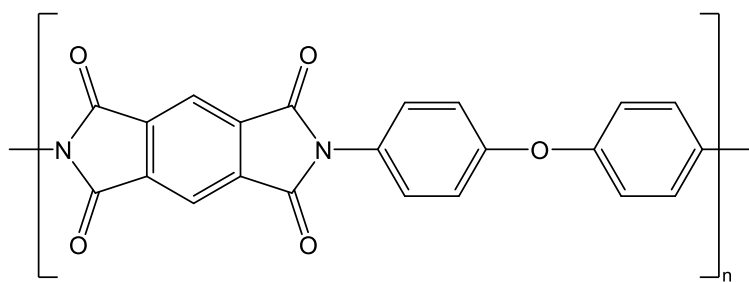


Figure S14. The color coordinates of the corresponding devices with different TeO_2 thicknesses based on simulation results.



Polyimide

Figure S15. The chemical structure of polyimide.

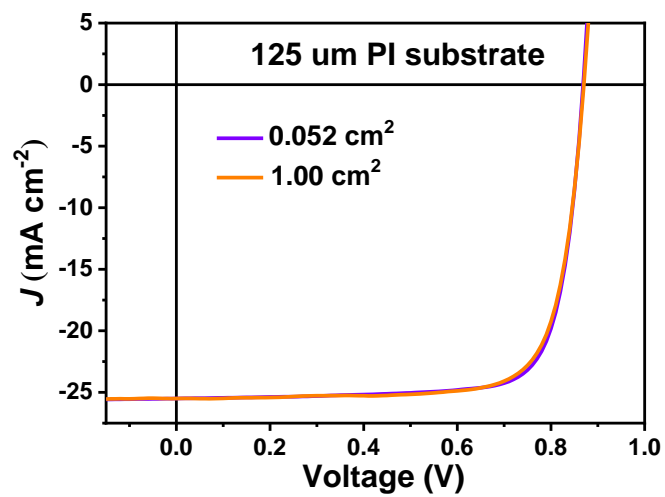


Figure S16. The J - V characteristics of 0.052 cm² and 1.00 cm² flexible OPVs based on 125 μm PI as substrate.

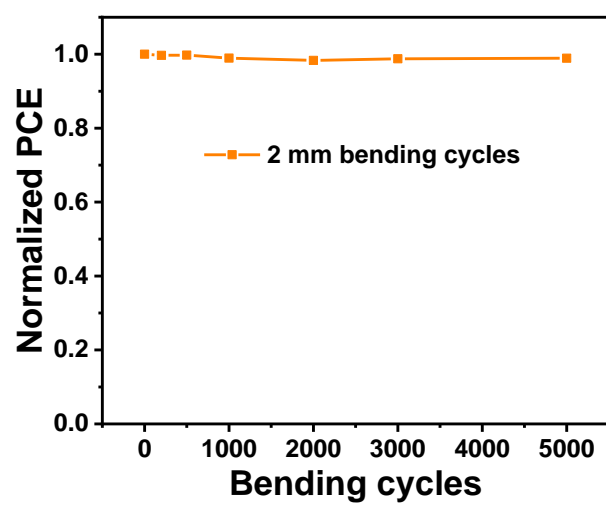


Figure S17. Normalized PCEs of 2 mm bending-tested flexible OPV device based on 125 μm PI as substrate.

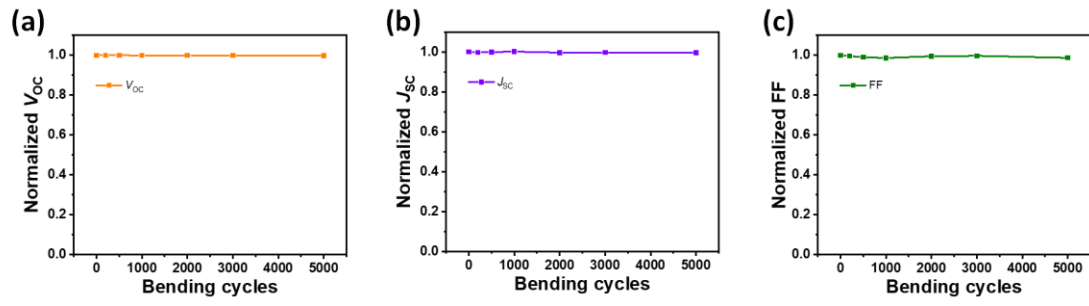


Figure S18. Normalized (a) V_{oc} , (b) J_{sc} and (c) FFs of 2 mm bending-tested flexible OPV devices based on 125 μm PI as substrate.

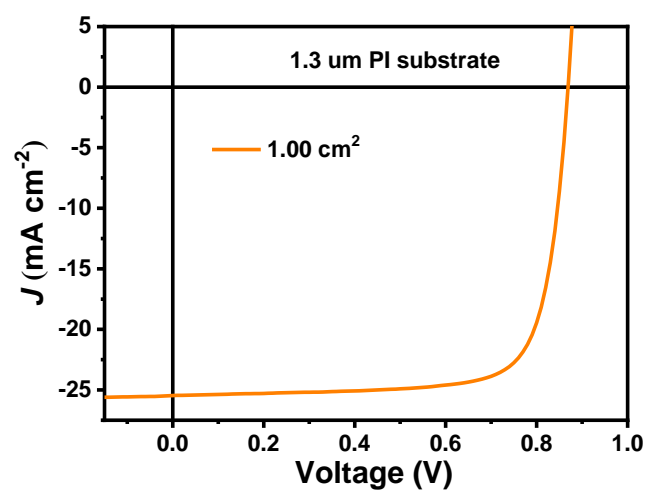


Figure S19. The J - V characteristics of 1.00 cm^2 ultra-flexible OPV device based on $1.3 \text{ }\mu\text{m}$ PI as substrate.

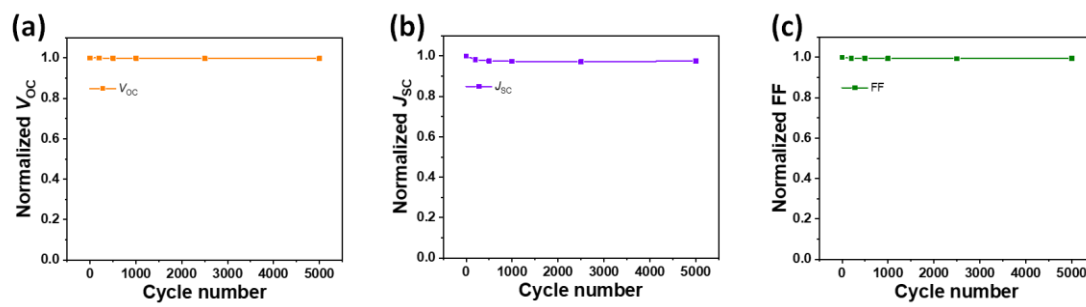


Figure S20. Normalized (a) V_{oc} , (b) J_{sc} and (c) FFs of compression-stretching deformation cycles with 30% compression of the ultra-flexible OPV.

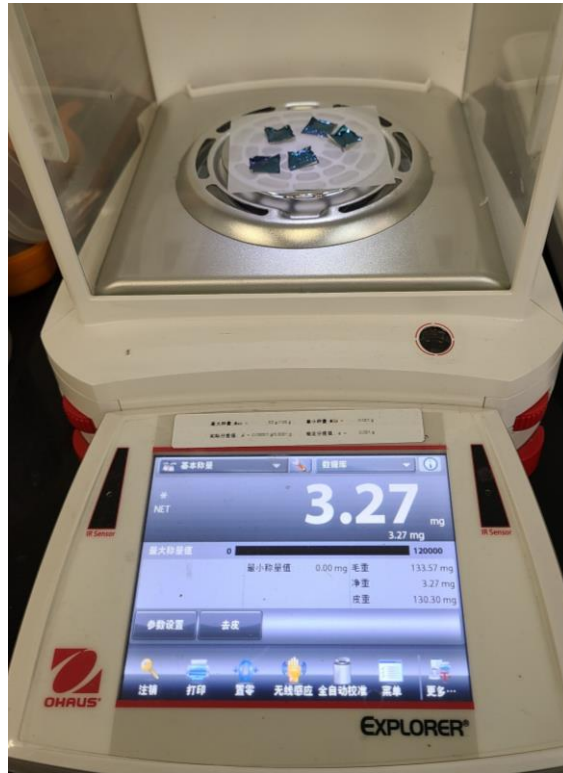


Figure S21. The weight of five 1.5 cm by 1.5 cm sizes ultra-flexible OPVs.



Figure S22. The length measurement of 1.5 cm by 1.5 cm sizes ultra-flexible OPVs (unpeeling off).

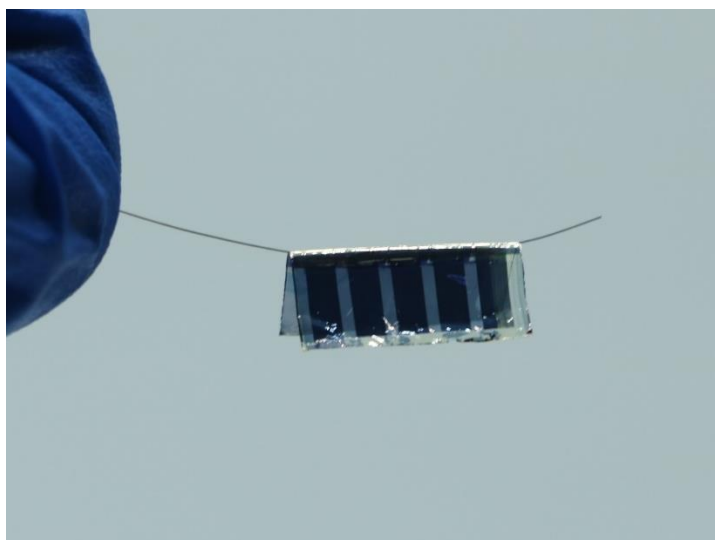


Figure S23. The display of an ultra-flexible OPV device on a single human hair.

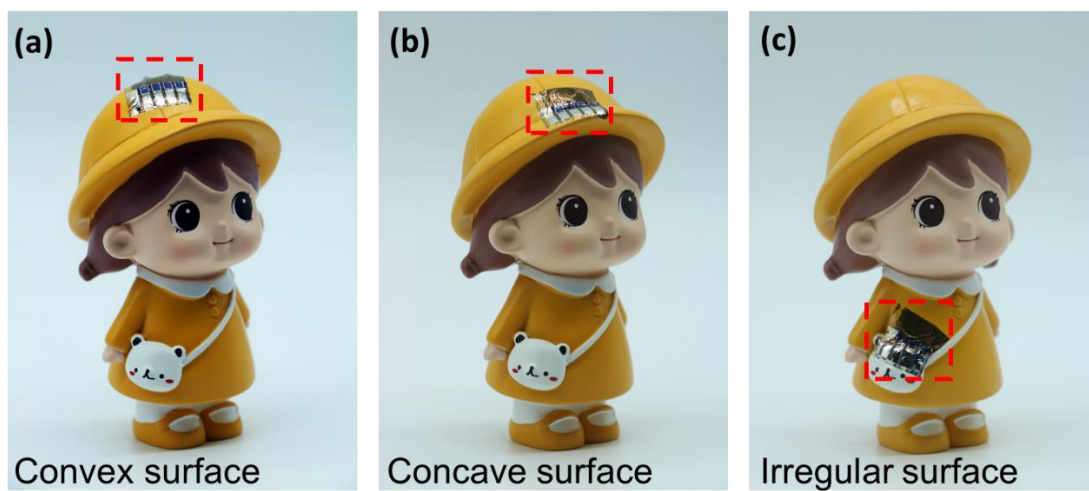


Figure S24. The display of ultra-flexible OPV device on the concave, convex, and irregular surfaces.

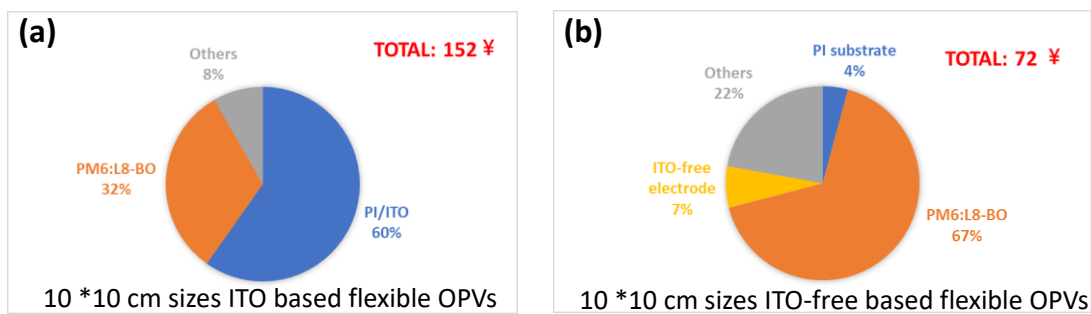


Figure S25. The cost analysis of (a) ITO and (b) ITO-free (Au/Ag) based 10*10 cm sizes flexible OPV devices.

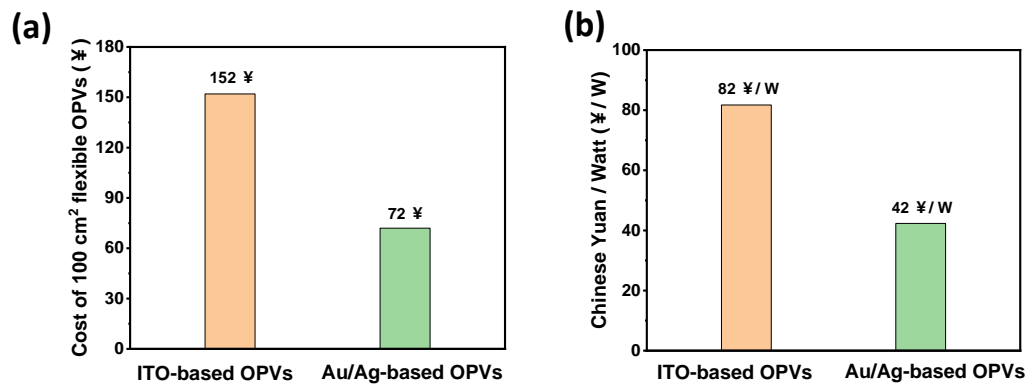


Figure S26. (a) The cost statistics of ITO and ITO-free (Au/Ag) based 10*10 cm sizes flexible OPV devices. (b) The cost-watt (¥/W) statistics of ITO-based and Au/Ag-Based flexible OPVs.

Supplemental Tables

Table S1. Transmittances, sheet resistances, and photovoltaic performances of 0.052 cm² devices with different ultra-thin Ag thicknesses. The \pm refers to the standard deviation.

Ag thicknesses [nm]	Sheet resistance [Ω /sq]	Transmittance at 565 nm [%]	V _{oc} [V]	J _{sc} [mA cm ⁻²]	J _{cal} [mA cm ⁻²]	FF [%]	PCE [%]
9	15.9	86.7	0.869	24.06	23.41	76.75	16.01 (15.86 \pm 0.13)
11	8.9	92.5	0.870	24.97	24.29	78.34	17.02 (16.89 \pm 0.08)
13	6.1	88.3	0.869	23.15	22.78	78.49	15.79 (15.68 \pm 0.09)

Table S2. Photovoltaic performances of the rigid OPVs with different ETLs and transparent electrodes. The \pm refers to the standard deviation.

ETLs	Transparent electrodes	Area [cm ²]	V _{oc} [V]	J _{sc} [mA cm ⁻²]	J _{calc.} [mA cm ⁻²]	FF [%]	PCE [%]
PFN-Br	9 nm Ag	0.052	0.767	21.03	20.44	63.22	10.20 (9.79±0.27)
PDINO	9 nm Ag	0.052	0.795	23.91	23.46	59.19	11.28 (10.85±0.32)
Bis-FIMG	9 nm Ag	0.052	0.869	24.06	23.41	76.75	16.01 (15.86±0.13)
Bis-FIMG	1 nm Au / 8 nm Ag	0.052	0.870	25.52	24.96	78.87	17.50 (17.45±0.05)
Bis-FIMG	1 nm Au / 8 nm Ag	1.00	0.869	25.59	-	77.36	17.20 (17.04±0.15)

Table S3. Photovoltaic performances of the flexible OPV tested by bending cycles with a radius of 2 mm based on 125 μm PI as substrate.

Bending cycles [times]	V_{oc} [V]	J_{sc} [mA/cm ²]	FF [%]	PCE [%]
0	0.861	25.49	77.56	17.02
200	0.860	25.41	77.25	16.90
500	0.861	25.46	76.79	16.83
1000	0.860	25.53	76.53	16.81
2000	0.861	25.39	77.17	16.86
3000	0.860	25.42	77.34	16.91
5000	0.859	25.38	76.57	16.72

Table S4. Photovoltaic performances and colors of the rigid OPVs with 15 nm, 25 nm and 75 nm TeO₂. The \pm refers to the standard deviation.




TeO ₂ thicknesses [nm]	Device color	Color coordinate	V _{oc} [V]	J _{sc} [mA cm ⁻²]	FF [%]	PCE [%]
15		0.3524, 0.2284	0.870	21.21	78.24	14.43 (14.15 \pm 0.16)
25		0.3359, 0.1926	0.870	23.15	78.43	15.80 (15.57 \pm 0.14)
75		0.2756, 0.2459	0.867	23.29	78.70	15.90 (15.68 \pm 0.13)

Table S5. Photovoltaic performances of the ultra-flexible OPV tested by compression-stretching deformation cycles with 30% compression.

Cycle number	V_{oc}	J_{sc}	FF	PCE
[times]	[V]	[mA/cm ²]	[%]	[%]
0	0.858	25.43	77.63	16.94
200	0.858	24.97	77.18	16.54
500	0.857	24.81	77.32	16.44
1000	0.857	24.76	77.20	16.38
2500	0.856	24.71	77.12	16.31
5000	0.856	24.79	77.26	16.39

Table S6. The statistical data for ultra-flexible OPVs.

Substrate thickness [μm]	Area [cm^2]	Device structure	PCE [%]	Ref.
3.0	0.04	Parylene/SU8/ITO/ZnO/ PBDTTT-OFT:IEICO-	13.0	1
3.0	1.0	4F:PC ₇₁ BM/MoO ₃ /Ag	11.6	1
6.0	0.0289	Ag NWs@PI-ZnO/ZnO/PM6:BTP-4Cl/MoO ₃ /Ag	13.55	2
7.0	0.0289	Ag NWs@HB-PI/ZnO/PM6:BTP-4Cl/MoO ₃ /Ag	13.52	3
3.0	0.04	Parylene/ITO/ZnO/PBDTTT-OFT: PC ₇₁ BM/MoO ₃ /Ag	10.67	4
1.4	0.04	Parylene/ITO/ZnO/PBDTTT-OFT: IEICO-4F/PEDOT:PSS/Ag	10.4	5
2.5	0.04	PET/D-PEDOT:PSS/PEDOT:PSS/PM6:Y6:PC71BM/PFNDI- Br/Ag	15.5	6
1.0	0.04	Parylene/ITO/ZnO/PNTz4T: PC ₇₁ BM/MoO ₃ /Ag	7.9	7
3.0	0.04	Parylene/ITO/ZnO/PBDTTT-OFT: PC ₇₁ BM/MoO ₃ /Ag	10.6	8
1.3	0.041	PEN/Ag NWs/PEI-Zn/PM6:IT-4F/MoO ₃ /Ag	10.4	9
1.3	0.041	PEN/PEDOT:PSS/PEI-Zn/PM6:IT-4F/MoO ₃ /Ag	12.9	9
1.3	0.041	PEN/Ag NWs/PEI-Zn/PM6:Y6/MoO ₃ /Ag	12.3	9
1.3	0.041	PEN/PEDOT:PSS/PEI-Zn/PM6:Y6/MoO ₃ /Ag	15.03	9
1.3	1.0	PEN/PEDOT:PSS/PEI-Zn/PM6:Y6/MoO ₃ /Ag	11.2	9
1.3	0.04	PI/ITO/ZnO/PTzNTz-BOBO:PC ₇₁ BM/MoO ₃ /Ag	9.3	10
3.0	0.04	tPI/ITO/PEI-Zn/PM6:Y6/MoO ₃ /Ag	15.8	11
1.3	0.052	PI/Ag/PCP-2F-Li/PEDOT:PSS/PM6:L8-BO/Bis-	17.52	This work
1.3	1.0	FIMG/Au/Ag/TeO ₂	17.08	This work

Table S7. The statistical data of power-per-weight for difference PV technologies.

PV technologies	Device structure	PCE [%]	Power per weight [W g ⁻¹]	Ref.
GaAs	Ga _{0.51} In _{0.49} P/GaAs/Ga _{0.73} In _{0.27} As	30.9	3.0	12
Quantum Dots	PET/parylene/graphene/oCVD	7.10	12.3	13
	PEDOT/Pbs-EDT/Pbs-TBAI/LiF/Al			
Perovskite	Parylene/ITGZO/PTAA/Perovskite/PCB	20.2%	30.3	14
	M/BCP/Cu			
Organic	tPI/ITO/PEI-Zn/PM6:Y6/MoO ₃ /Ag	15.80	33.80	11
Organic	PI/Ag/PCP-2F-Li/PEDOT:PSS/PM6:L8-BO/Bis-FIMG/Au/Ag/TeO ₂	17.32	39.72	This work

Table S8. The cost statistics of 10*10 cm sizes ITO-based flexible OPV devices

Materials	Price per unit	Dosage	Price (¥)	Content (%)
PI/ITO	9000 ¥ / m ²	100 cm ²	90	59.2
PEDOT:PSS	1000 ¥/ 1000 mL	0.2 mL	2	1.3
PM6	22000 ¥/ g	1.5 mg	33	21.7
L8-BO	8000 ¥/ g	1.8 mg	15	9.9
PDINN	7600 ¥/ g	0.2 mg	1.5	1.0
Ag	7 ¥/ g	0.64 g	4.5	3.0
Others	\	\	6	3.9
Total	\	\	152	100

Table S9. The cost statistics of 10*10 cm sizes ITO-free flexible OPV devices.

Materials	Price per unit	Dosage	Price (¥)	Content (%)
PI	300 ¥/ m ²	100 cm ²	3	4.2
PEDOT:PSS	1000 ¥/ 1000 mL	0.2 mL	2	2.8
PM6	22000 ¥/ g	1.5 mg	33	45.8
L8-BO	8000 ¥/ g	1.8 mg	15	20.8
Bis-FIMG	7600 ¥/ g	0.2 mg	1.5	2.1
Ag	7 ¥/ g	0.7 g	4.9	6.8
Au	500 ¥/ g	10 mg	5	6.9
TeO ₂	10 ¥/ g	10 mg	0.1	0.1
PCP-2F-Li	8000 ¥/ g	0.2 mg	1.6	2.2
Others	\	\	6	8.3
Total	\	\	72.1	100

Supplementary References

1. W. Huang, Z. Jiang, K. Fukuda, X. Jiao, C. R. McNeill, T. Yokota and T. Someya, *Joule*, 2020, **4**, 128.
2. Y. Wang, Q. Chen, G. Zhang, Y. Wang, Z. Zhang, J. Fang, C. Zhao and W. Li, *Chem. Eng. J.*, 2023, **451**, 138612.
3. Y. Wang, Q. Chen, Y. Wang, G. Zhang, Z. Zhang, J. Fang, C. Zhao and W. Li, *Macromol. Rapid Commun.*, 2022, 2200432.
4. S. Park, S. W. Heo, W. Lee, D. Inoue, Z. Jiang, K. Yu, H. Jinno, D. Hashizume, M. Sekino, T. Yokota, K. Fukuda, K. Tajima and T. Someya, *Nature*, 2018, **561**, 516.
5. S. I. Rich, S. Lee, K. Fukuda and T. Someya, *Adv. Mater.*, 2022, **34**, 2106683.
6. W. Song, K. Yu, E. Zhou, L. Xie, L. Hong, J. Ge, J. Zhang, X. Zhang, R. Peng and Z. Ge, *Adv. Funct. Mater.*, 2021, **31**, 2102694.
7. H. Jinno, K. Fukuda, X. Xu, S. Park, Y. Suzuki, M. Koizumi, T. Yokota, I. Osaka, K. Takimiya and T. Someya, *Nat. Energy*, 2017, **2**, 780.
8. H. Jinno, T. Yokota, M. Koizumi, W. Yukita, M. Saito, I. Osaka, K. Fukuda and T. Someya, *Nat. Commun.*, 2021, **12**, 2234.
9. F. Qin, W. Wang, L. Sun, X. Jiang, L. Hu, S. Xiong, T. Liu, X. Dong, J. Li, Y. Jiang, J. Hou, K. Fukuda, T. Someya and Y. Zhou, *Nat. Commun.*, 2020, **11**, 4508.
10. H. Kimura, K. Fukuda, H. Jinno, S. Park, M. Saito, I. Osaka, K. Takimiya, S. Umezumi and T. Someya, *Adv. Mater.*, 2019, **31**, 1808033.
11. S. Xiong, K. Fukuda, S. Lee, K. Nakano, X. Dong, T. Yokota, K. Tajima, Y. Zhou and T. Someya, *Adv. Sci.*, 2022, **9**, 2105288.
12. J. Schön, G. M. M. W. Bissels, P. Mulder, R. H. van Leest, N. Gruginskie, E. Vlieg, D. Chojniak and D. Lackner, *Prog. Photovoltaics*, 2022, **30**, 1003.
13. M. M. Tavakoli, M. H. Gharahcheshmeh, N. Moody, M. G. Bawendi, K. K. Gleason and J. Kong, *Adv. Mater. Interface*, 2020, **7**, 2000498.
14. J. Wu, P. Chen, H. Xu, M. Yu, L. Li, H. Yan, Y. Huangfu, Y. Xiao, X. Yang, L. Zhao, W. Wang, Q. Gong and R. Zhu, *Sci. China Mater.*, 2022, **65**, 2319.